Structural Study of BSA/Poly(ethylene glycol) Lipid Conjugate Complexes

Valeria Castelletto,* Marta J. Krysmann, Luke A. Clifton, and John Lambourne

School of Chemistry, Food Biosciences and Pharmacy, The University of Reading, P.O. BOX 226, Whiteknights, Reading RG6 6AP, United Kingdom

Laurence Noirez

Laboratoire Léon Brillouin, CEA-Saclay, 91191 Gif-sur-Yvette Cedex, France

Received: June 7, 2007; In Final Form: July 12, 2007

In this work we report the structural characteristics of bovine serum albumin/poly(ethylene glycol) lipid conjugate (BSA/PEG_{2000}−PE) complexes under physiological conditions (37 °C and pH 7.4) for particular fractions of BSA to PEG−lipid concentration, $c_{BSA}/c_{PEG_{2000}-PE}$. Ultraviolet fluorescence spectroscopy (UV) results shown that PEG_{2000}−PE is associated to BSA, leading to protein unfolding for fixed $c_{BSA} = 0.01$ wt % and variable $c_{PEG_{2000}-PE} = 0.0015-0.6$ wt %. Tryptophan groups on the BSA surface are in contact with the PEG−lipid at $c_{PEG_{2000}-PE} = 0.0015$ wt %, while they are exposed to water at $c_{PEG_{2000}-PE} > 0.0015$ wt %. Dynamic and static light scattering (DLS and SLS) and small-angle neutron scattering (SANS) point out the existence of individual BSA/PEG−lipid complexes in the system for fixed $c_{BSA} = 1$ wt % and variable $c_{PEG_{2000}-PE} = 0.15-2$ wt %. DLS shows that there is only one BSA molecule per protein/PEG−lipid complex, while SLS shows that the PEG−lipid associates to the BSA without promoting aggregation between adjacent protein/polymer−lipid conjugate complexes. SANS was used to show that BSA/PEG_{2000}−PE complexes adopt an oblate ellipsoidal shape. Partially unfolded BSA is contained in the core of the oblate ellipsoid, which is surrounded by an external shell containing the PEG_{2000}−PE.

Introduction

The modification of blood proteins to enhance the natural functions of blood has been the subject of research with the aim to prevent organ dysfunctions associated with capillary blood leak into tissues.[1] The blood plasma protein serum albumin is a protein that maintains the "osmotic pressure" that causes fluid to remain within the blood stream instead of leaking out into tissues. Fluid resuscitation techniques can be used to stabilize blood disorders consisting of a decrease in the volume of circulating blood.[2] In particular, the administration of serum albumin covalently linked to poly(ethylene glycol) (PEG)[3] as a resuscitative agent has proved to be potentially effective in clinical treatment of syndromes associated with capillary blood leaks into tissue.[1,2]

Although potentially effective, the use of serum albumin covalently linked to PEG is not commonly used to reduce capillary blood leaks, since the present coupling methods can lead to the presence of PEG−serum albumin contaminated with unreacted active PEG and coproduct.[1] Therefore, the formulation of alternative procedures to increase the osmotic pressure in the blood stream is attracting great attention. A possibility is the preparation of albumin/polyethylene glycol−lipid complexes.

In a previous work[4] we reported the formation of complexes by self-assembly of bovine serum albumin (BSA) with the poly(ethylene glycol) lipid conjugate 1,2-distearoyl-*sn*-glycero-3-phosphoethanolamine-*N*-[methoxy(polyethylene glycol)-2000], namely PEG_{2000}−PE, in phosphate saline buffer solution (pH 7.4) at 20 °C. BSA was chosen due to the extensive information available on BSA properties in solution[5−7] and because it can be produced at industrial scale. Dynamic light scattering (DLS) results showed that the polymer−lipid conjugate associates to the BSA leading to the formation of BSA/PEG_{2000}−PE complexes with a size intermediate between a BSA monomer and a PEG_{2000}−PE micelle.[4] Rheology suggested that BSA/PEG_{2000}−PE complexes might be surrounded by a relatively compact PEG−lipid shell. Ultraviolet fluorescence spectroscopy (UV) and circular dichroism denoted BSA unfolding for high PEG_{2000}−PE concentrations without a noticeable variation in the α helix content of the protein secondary structure.[4]

In this work we are going to study the stability and structural characteristics of BSA/PEG_{2000}−PE complexes under physiological conditions (37 °C and pH 7.4), as a first step to define these complexes as good candidates for designed osmotic blood pressure regulators. It is desirable that individual BSA/PEG_{2000}−PE complexes can be identified in the system at 37 °C and that the tertiary structure of the BSA is not noticeably altered under association with the PEG_{2000}−PE. This new study is necessary because the results mentioned above for 20 °C might differ from those obtained at 37 °C, since higher temperatures can destabilize the BSA/PEG_{2000}−PE complexes leading to the formation of a protein/polymer−lipid conjugate network throughout the system. In addition, our previous studies at 20 °C do not provide detailed information about the structure of the complexes. In this work, UV will be used to monitor the association of PEG_{2000}−PE to BSA. DLS will give information about the average size of the BSA/PEG_{2000}−PE complexes. Evidence of protein network formation will be investigated by DLS and static light scattering (SLS). Finally, small-angle neutron scattering (SANS) will be used to provide detailed information about the

* Address correspondence to this author. Phone: 44 113 343 7595. Fax: 44 113 343 6551. E-mail: v.castelletto@reading.ac.uk.

10.1021/jp074409n CCC: $37.00
Published on Web 09/06/2007

tertiary structure adopted by the BSA in the complex as well as the location of the PEG−lipid conjugate within the complex.

Experimental Section

Materials. BSA (M_{BSA}= 66 000 g mol^{-1}) and phosphate buffer saline (PBS, pH 7.4, ionic strength I = 0.169 M) were purchased from Sigma (U.S.A.), while PEG_{2000}−PE ($C_{133}H_{267}N_2O_{55}P$, $M_{PEG_{2000}-PE}$ = 2806 g mol^{-1}) was obtained from Avanti Polar Lipids (U.S.A.).

To prepare the samples, the PEG_{2000}−PE was first diluted in the solvent by stirring the solution for 2 h. Then, the BSA was added to the PEG_{2000}−PE solution and the ternary sample was stirred for a further 30 min. The shear rate used for stirring the samples was 0.6 s^{-1}. Samples contained amounts of PEG_{2000}−PE and BSA corresponding to several fractions $\Delta = c_{PEG_{2000}-PE}/c_{BSA}$, where each concentration c was measured in g/g. During the experiments, the parameter Δ was varied by keeping c_{BSA} constant and increasing $c_{PEG_{2000}-PEG}$.

Samples for DLS, SLS, and UV experiments were dissolved in PBS aqueous solutions, at pH 7.4. Samples used for SANS experiments were dissolved in pure D_2O, without PBS, since the absence of PBS in the solution increases the contrast improving the SANS signal.

Although PBS has pH 7.4 while D_2O has pH 7.0, results obtained for samples containing PBS can be compared to results obtained for samples prepared with D_2O. BSA conformation remains nearly constant for solutions with pH 7.0−7.4,[8,9] while the isoelectric point for BSA in solution is around pH 4.5,[10] so the net charge of the BSA is negative in the range pH 7.0−7.4. In addition, PEG_{2000}−PE is negatively charged in solution for pH 7.0−7.4.

In this work, a set of different experimental techniques have been used to study the formation of protein/PEG−lipid conjugate aggregates. We have observed in our previous studies of the BSA/PEG_{2000}−PE system[4] that different techniques are sensitive to different concentrations of BSA and therefore constrain the experiments to values of Δ with a particular c_{BSA}. Samples with fixed c_{BSA} = 0.01 wt % and variable $c_{PEG_{2000}-PEG}$ are in the Δ_1 range, and have been studied by UV. Samples studied by DLS, SLS, and SANS are in the Δ_2 range, with fixed c_{BSA} = 1 wt % BSA and variable $c_{PEG_{2000}-PEG}$. All experiments have been carried out at 37 °C.

DLS. Experiments were performed on an ALV CGS-3 system with 5003 multidigital correlator. The light source was a 20 mW He−Ne laser, linearly polarized, with λ = 633 nm. Scattering angles in the range 40 ° ≤ θ ≤ 150° were used for all the experiments. Samples were filtered through 0.20 μm Anotop filters from Whatman into standard 0.5 cm diameter cylindrical glass cells.

SLS. The SLS was measured by using the same experimental setup described for DLS above, but fixing the scattering angle to 90°. A total of 255 intensity readings were obtained and averaged to provide the intensity scattered at 90°, I(90°).

SANS. Experiments were conducted at the Laboratoire Léon Brillouin (CEA-CNRS), using the SANS instrument PAXY with a two-dimensional detector, comprising 128 × 128 cells of 5 × 5 mm^2 size. A wavelength λ = 5 or 12 Å and a sample−detector distance of 2.4 m were chosen to measure the SANS curves. Measurements were carried out at 37 °C. Solutions were poured into sealed 1 mm path length standard quartz cuvettes.

The data from the two-dimensional area detector were converted into one-dimensional intensity profiles by radial averaging. The SANS data were then corrected to allow for sample transmission and background scattering (using a D_2O sample as reference). The resulting solvent-corrected intensity is denoted $I(q)$.

UV. The emission spectrum of BSA, at an excitation wavelength of 280 nm, was recorded with a Perkin-Elmer LS50B Luminescence Spectrometer. Samples were mounted in 5 mm path length quartz cuvettes. Emission spectra were obtained from 200 to 800 nm, using 60 s collection time.

Theory

DLS. DLS experiments measured the intensity correlation function of the radiated light $g^{(2)}(q,t)$:[11]

$$g^{(2)}(q,t) = 1 + A[g^{(1)}(q,t)]^2 \quad (1)$$

where A accounts for a correction factor depending on the alignment of the instrument, $q = [4\pi n \sin(\theta/2)]/\lambda$ is the scattering vector (λ = vacuum wavelength of the radiation and n = refractive index of the medium), t is the delay time, and $g^{(1)}(q,t)$ is the electric field correlation function.

The relaxation rate distribution of the system, $G(\Gamma)$, can be calculated through the modeling of the electric field correlation function according to:[12]

$$g^{(1)}(t) = \int_0^\infty G(\Gamma) \exp(-\Gamma t)\, d\Gamma \quad (2)$$

The inverse Laplace transform in eq 2 provides a tool for calculating the diffusion coefficient of the system. The relaxation rate distributions for different scattering vectors can be used to construct a plot of $\bar{\Gamma}$ vs q^2 (where, for a unimodal distribution, $\bar{\Gamma}$ is taken as the decay rate corresponding to the maximum in $G(\Gamma)$). The mutual diffusion coefficient is calculated as the slope $D = \bar{\Gamma}/q^2$ and it enables the apparent hydrodynamic radius R_H to be calculated according to the Stokes−Einstein equation:

$$R_H = \frac{k_B T}{6\pi\eta D} \quad (3)$$

where k_B= 1.38 × 10^{-23} J K^{-1} is the Boltzmann constant and η is the viscosity of water, taken to be η = 7.0 × 10^{-4} Pa s at 37 °C.

SANS. The coherent part of the SANS intensity from an isotropic solution of globular objects, $I(q)$, can be written as:[13]

$$I(q) = kP(q)S(q) \quad (4)$$

where k is a normalization constant proportional to the number density of scatterers, $P(q)$ is the form factor, $S(q)$ is the structure factor, and q is the scattering vector given by $q = 4\pi \sin(\theta/\lambda)$. The systems studied in this work correspond to widely separated systems. Therefore $S(q) \approx 1$ in eq 4, so $I(q)$ is proportional to the form factor $P(q)$.

The form factor $P(q)$ for the PEG_{2000}−PE micelles was fitted to a system of polydisperse spheres with homogeneous scattering length distribution:[14]

$$P(q) = \int_0^\infty \Phi(q,r) f(R)\, dr \quad (5)$$

where $\Phi(q,r)$ is the scattering function of a sphere:

$$\Phi(q,r) = 3[\sin(qr) - qr\cos(qr)]/(qr)^3 \quad (6)$$

and $f(R)$ accounts for a Gaussian distribution of micellar radius, with mean radius $\bar{R}$, and width ∂:

$$f(R) = (2\pi\partial^2)^{-1/2} \exp[-(r - \bar{R})^2/2\partial^2] \quad (7)$$

$P(q)$ for the sample containing 1 wt % of BSA, free of polymer−lipid conjugate, was fitted to a triaxial ellipsoid with half axis (a, b, c):[15]

$$P(q) = \frac{2}{\pi}\int_0^{\pi/2}\int_0^{\pi/2} \Phi^2[q,r(a,b,c,\varphi,\theta)] \sin\varphi \, d\varphi \, d\theta \quad (8)$$

with

$$r(a,b,c,\varphi,\theta) = [(a^2\sin^2\theta + b^2\cos^2\theta)\sin^2\varphi + c^2\cos^2\varphi]^{1/2} \quad (9)$$

Samples containing BSA and PEG_{2000}−PE where fitted to an ellipsoid of revolution with two different levels of scattering length density. The ellipsoid consists of an inner core, with half axis (t, $s = \nu t$, $s = \nu t$, $\nu < 1$: inner core anisometry), surrounded by an external shell with thickness d. In this model it is assumed that the BSA is contained in the core of the ellipsoid, while the external shell is made by the PEG_{2000}−PE molecules associated to the BSA:[16]

$$P(q) = \frac{2}{\pi}\int_0^{\pi/2} \{(\rho_c - \rho_{sh})V_c\Phi[2\pi q t g_1(\theta)] + (\rho_{sh} - \rho_s)V_{el}\Phi[2\pi(t+d)g_2(\theta)]\}^2 \cos\theta \, d\theta \quad (10)$$

where

$$g_1(\theta) = [\cos^2(\theta) + \nu^2\sin^2(\theta)]^{1/2} \quad (11a)$$

$$g_2(\theta) = [\cos^2(\theta) + \nu'^2\sin^2(\theta)]^{1/2} \quad (11b)$$

The constants ρ_c, ρ_{sh}, and ρ_s in eq 10 are the scattering length densities of the core, the shell, and the solvent, respectively, while $\nu' = (s + d)/(t + d)$. Eq 10 also depends on the ellipsoid core volume, $V_c = 4\pi s^2 t/3$, and the total ellipsoid volume, $V_{el} = [4\pi(s + d)^2(t + d)]/3$.

The SANS data in our work have not been measured in absolute units. Therefore, the fraction $(\rho_c - \rho_{sh})/(\rho_{sh} - \rho_s)$ is relevant to the fitting of the experimental data using eq 10, instead of the terms $(\rho_c - \rho_{sh})$ and $(\rho_{sh} - \rho_s)$. If the BSA undergoes unfolding due to the interaction with the PEG−lipid conjugate, it is expected that V_c contains some water, associated to the loose structure of BSA. Similarly, the shell of the ellipsoid in eq 10 has to contain water due to the presence of the highly hydrophilic PEG_{2000} block. Our model allows for water in the core and the shell of the ellipsoid by writing

$$\rho_c = (1 - X_c)\rho_{BSA} + X_c\rho_{D_2O} \quad (12a)$$

$$\rho_{sh} = (1 - X_{sh})\rho_{PEG_{2000}-PE} + X_{sh}\rho_{D_2O} \quad (12b)$$

where $\rho_{BSA} = 3.89 \times 10^{-6}$ Å^{-2},[17] $\rho_{PEG_{2000}-PE} = 1.65 \times 10^{-7}$ Å^{-2}, and $\rho_{D_2O} = 6.36 \times 10^{-6}$ Å^{-2} are the scattering length densities of the BSA, PEG_{2000}−PE, and D_2O, respectively. The parameters X_c and X_{sh} are the fraction of water contained in the core and the shell, respectively.

The model used to fit the SANS data for the PEG_{2000}−PE micelles (eqs 5−7) has two parameters: the mean radius $\bar{R}$ and the width ∂. The model to fit the SANS curve for the pure BSA solution (eqs 8 and 9) has three parameters: the half-axes a, b, and c. $P(q)$ for the BSA/PEG_{2000}−PE complexes (eqs 10−12) has four parameters: the half-axis t, the shell thickness d, the anisometry ν, and the fraction $(\rho_c - \rho_{sh})/(\rho_{sh} - \rho_s)$. The parameters X_c and X_{sh} are calculated from the fitted $(\rho_c - \rho_{sh})/(\rho_{sh} - \rho_s)$ fraction by using eqs 12a and 12b.

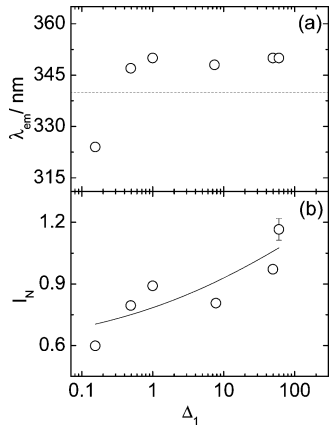

Figure 1. (a) UV emission wavelength measured as a function of Δ_1 for aqueous BSA + PEG_{2000}−PE solutions. The dotted lines correspond to the emission wavelength measured for $\Delta_1 = 0$. (b) UV intensity measured for $\Delta_1 > 0$, normalized by the UV intensity measured for $\Delta_1 = 0$. The experimental error is shown for $\Delta_1 = 60$. The full line is a guide for the eyes.

For diluted systems, the scattering at low q obeys the Guinier law:[18]

$$\lim_{q\to 0} I(q) = I(0)\exp\left(-\frac{q^2 R_{g,G}{}^2}{3}\right) \quad (13)$$

where $I(0)$ is the scattering at $q = 0$. $R_{g,G}$ in eq 13 can be evaluated from a $\ln[I(q)]$ vs q^2 Guinier plot in the regime $qR_{g,G} < 1$.

The information extracted from eq 13 can be complemented by calculating the distance distribution function $p(r)$ given by:[19]

$$p(r) = \frac{r^2}{2\pi}\int_0^\infty \frac{I(q)q^2\sin(qr)}{qr} \, dq \quad (14)$$

which provides information about the shape of the particle and goes from zero for distances higher than the maximum diameter of the particle D_{max}. The $p(r)$ function also provides the value of the radius of gyration of the particle through the integral relation:[19]

$$R_{g,I}{}^2 = \frac{\int_0^\infty p(r)r^2 \, dr}{2\int_0^\infty p(r) \, dr} \quad (15)$$

Results and Discussion

The UV fluorescence of tryptophan (Trp) groups in the BSA has been widely used in the literature to probe conformational changes in that protein.[20−24] The emission wavelength of Trp in water corresponds to $\lambda_{em} = 350$ nm, while lower values are measured for the Trp exposed to a hydrophobic environment.[21,22] In addition, it is known that changes in fluorescence intensity emission of Trp groups denote BSA unfolding.[21,22]

UV experiments were performed on samples containing 0.01 wt % of BSA with $\Delta_1 = 0-60$. Following UV experiments on the BSA/PEG_{2000}−PE system at 20 °C,[4] the Trp excitation wavelength was fixed to $\lambda_{ex} = 280$ nm. The UV output signal obtained for all the samples was characterized by an unimodal emission peak, centered in λ_{em} and with intensity I_{uv}. Figure 1a shows the emission wavelength λ_{em} measured for $\Delta_1 = 0-60$,

while Figure 1b shows the normalized reciprocal intensity $I_N = I_{uv,o}/I_{uv}$ measured for $\Delta_1 = 0.15-60$ ($I_{uv,o}$: UV intensity emission peak measured for $\Delta_1 = 0$).

Figure 1a shows $\lambda_{em} = 340$ nm for $\Delta_1 = 0$, while there are two different regimes in λ_{em} for $\Delta_1 > 0$. For $\Delta_1 = 0.15$, there is a blue shift of the $\lambda_{em} = 340$ nm measured for free BSA. The blue shift indicates that the Trp groups are exposed to a hydrophobic environment (probably consisting of the PE blocks) and can be associated to the formation of H-bonds between the Trp groups and the PEG−lipid conjugate.[24] In contrast, Figure 1a shows that for $\Delta_1 > 0.15$ there is a red shift of the $\lambda_{em} = 340$ nm measured for free BSA. It is known that surfactants can unfold BSA.[21] Therefore, the red shift could be due to the unfolding of the BSA molecule, which subsequently means that the Trp groups are more likely to be exposed to the aqueous solution.

Figure 1b shows that I_N increases upon increasing Δ_1, outside the experimental error, denoting a progressive unfolding of the BSA upon increasing $c_{PEG_{2000}-PE}$. It is worthy to point out that $I_N \neq 1$ at $\Delta_1 = 0.15$, which denotes a partial unfolding of BSA, even if the Trp groups are not exposed to water, as denoted by the blue shift in λ_{em} observed at $\Delta_1 = 0.15$ (Figure 1a).

According to the UV results, PEG_{2000}−PE association to the BSA induces protein unfolding. To probe the potential application of the BSA/PEG_{2000}−PE complexes as osmotic pressure control agents, it is necessary to verify that BSA unfolding does not lead to the formation of a protein/polymer−lipid conjugate network throughout the system. Indeed, it is desirable that individual BSA/PEG_{2000}−PE complexes can be identified in the system despite the protein unfolding. This information can be obtained by undertaking DLS and SLS experiments.

DLS experiments were performed for samples contained 1 wt % of BSA with $\Delta_2 = 0-2$, and also for a sample free of protein, containing only 0.25 wt % of PEG_{2000}−PE. The CONTIN program was used to calculate the relaxation rate distributions $G(\Gamma)$ for $40° \leq \theta \leq 150°$. All the resulting $G(\Gamma)$ functions were dominated by only one peak. The position of the peak maximum in $G(\Gamma)$ was taken as the average relaxation rate, $\bar{\Gamma}$, of the system. The dependence of $\bar{\Gamma}$ on q^2 could be fitted with a straight line with an intercept of zero, indicating a diffusive process time. The apparent diffusion coefficient D was calculated from the gradient of the $\bar{\Gamma}$ vs q^2 plot, and the hydrodynamic radius R_H was then obtained with eq 3.

The dependence of D and R_H on Δ_2, for the samples containing BSA, is shown in Figure 2, parts a and b, respectively. R_H calculated for samples with 0.25 wt % PEG_{2000}−PE was 67 Å with a corresponding diffusion time of 4.77×10^9 $Å^2\ s^{-1}$ (results not shown).

The diffusion coefficient in Figure 2a decreases with increasing Δ_2, suggesting that the size of the BSA/PEG_{2000}−PE complexes increases upon increasing the polymer−lipid conjugate concentration.

Figure 2b shows that although R_H steadily grows from 35.6 (for 1 wt % of BSA with $\Delta_2 = 0$) to 48.4 Å (for 1 wt % of BSA with $\Delta_2 = 2$), it always remains lower than R_H measured for PEG_{2000}−PE micelles ($R_H = 67$ Å). R_H values support the idea that PEG_{2000}−PE conjugates do not self-associated in the presence of protein; instead the PEG−lipid conjugate is preferentially associated to the protein. The absence of multimodal apparent diffusion coefficients or extremely high R_H values (Figure 2a,b) denotes that the system does not present a network structure, and supports the idea that individual BSA/PEG_{2000}−PE complexes can be identified in the solution.

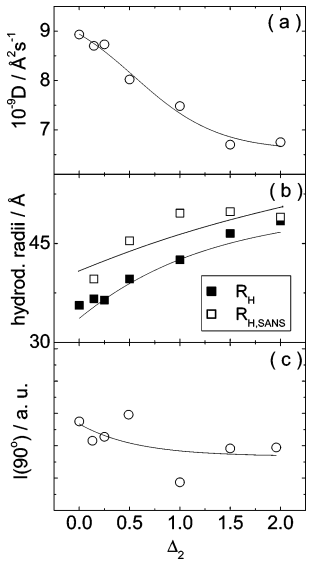

Figure 2. Light scattering results: dependence of (a) apparent diffusion coefficient D, (b) hydrodynamic radii, and (c) SLS intensity $I(90°)$ with Δ_2. The solid square symbols (■) in part b correspond to R_H measured by DLS, while the open square symbols (□) in part b correspond to $R_{H,SANS}$ calculated by using the parameters extracted from the fitting of the SANS curves to eqs 10−12. The full lines are a guide for the eyes.

As expected, the hydrodynamic radius obtained for $\Delta_2 = 0$, $R_H = 36$ Å is in good agreement with $R_H = 35$ Å reported by us in the literature for the same sample at 20 °C.[4] These values also closely match the hydrodynamic radius $R_H = 34$ Å reported for BSA in pH 7.2 buffer at room temperature.[8] R_H values for $\Delta_2 > 0$ (Figure 1b) are in average 20% smaller than the R_H radius previously measured by us for the same samples at 20 °C.[4] This result is consistent with an increase in hydrophobicity of the PEG_{2000} block at higher temperatures, which induces a folding of the polymer chain.

Data in Figure 2b show that R_H continuously increases with Δ_2. We have previously reported the stabilization of R_H upon increasing Δ_2 for $\Delta_2 > 1$ at 20 °C. It is evident from Figure 2b that a higher temperature (37 °C) does not allow the complexes to reach a stable configuration with a fixed R_H independent of Δ_2.

The self-association of BSA and human serum albumin (HSA) in solutions with pH ∼7 has been studied in the literature using light scattering.[25−27] The results obtained in those studies show a coexistence of serum albumin monomers (with $R_{H,M} \approx$ 36 Å) and dimmers (with $R_{H,D} \approx 48$ Å).[25,27] According to that information, Figure 2b shows that BSA/PEG_{2000}−PE complexes do not contain more than one BSA molecule (the maximum R_H for the BSA/PEG_{2000}−PE complexes is 48.4 Å, very close to $R_{H,D}$ for a pure BSA dimmer).

Figure 2c shows the SLS intensity $I(90°)$ measured in the range $\Delta_2 = 0-2$. The smooth variation of $I(90°)$ with Δ_2 is well defined (the experimental error for the intensity is about 1% of the measured $I(90°)$ value, falling within the symbols in Figure 2c) and does not denote the formation of a protein/polymer−lipid conjugate network upon BSA unfolding.

Figure 3 shows the SANS curve obtained for 0.15 wt % of PEG_{2000}−PE. The scattering data vary smoothly with q and do not present structure factor effects. The information in the SANS curve was not enough to differentiate the contrast of the PEG_{2000} block from the contrast of the PE block in the polymer−lipid conjugate micelle. However, a hard sphere model according to eqs 5−7 provided a satisfactory fitting to the experimental data.

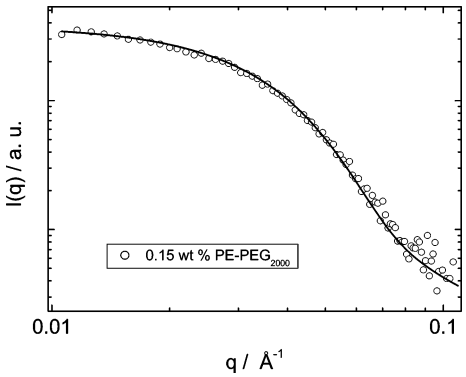

Figure 3. (○) SANS curve for 0.15 wt % PE−PEG_{2000}. The full line corresponds to the fitting according to eqs 5−7.

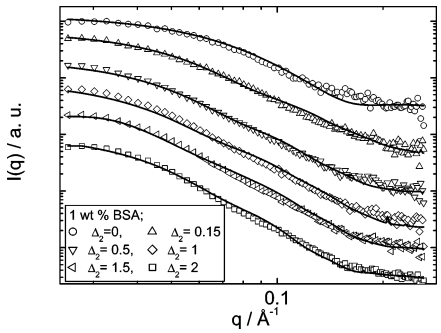

Figure 4. SANS curves for samples containing 1 wt % BSA and (○) $\Delta_2 = 0$, (△) $\Delta_2 = 0.15$, (▽) $\Delta_2 = 0.5$, (◇) $\Delta_2 = 1.0$, (rotated ▽) $\Delta_2 = 1.5$ or (□) $\Delta_2 = 2.0$. The SANS curves have been shifted to enable the visualization of the data. The full line in the inset is the modeling of the data according to eqs 8 and 9 ($\Delta_2 = 0$) or eqs 10−12 ($\Delta_2 = 0.15-2$).

TABLE 1: Parameters Extracted and Calculated from the Fitting of the SANS Curves Shown in Figure 4

Δ_2	a [Å]	b [Å]	c [Å]	t [Å]	s [Å]	d [Å]	ν	X_c [%]	X_{sh} [%]
0	23.4	21.9	53.0						
0.15				7.7	49.2	4.9	0.23	30	62
0.5				13.3	58.6	2.9	0.26	43	63
1				12.5	65.3	3	0.23	51	66
1.5				14.6	65	3	0.26	58	76
2				18.9	62.1	1.9	0.33	64	74

In good agreement with $R_H = 66$ Å obtained by DLS for PEG−lipid conjugates micelles, the fitting in Figure 3 provided a micellar radius $\bar{R} = 63$ Å with 40% polydispersity.

Figure 4 shows the SANS curves obtained for 1 wt % BSA and $\Delta_2 = 0-2$. Similarly to the result in Figure 3, SANS curves in Figure 4 do not show structure factor effects and decay smoothly with increasing q.

Following low-resolution models reported in the literature for BSA[8] the SANS curve measured for $\Delta_2 = 0$ was modeled according to a triaxial ellipsoid (eqs 8 and 9). The protein conformation for 1 wt % BSA and $\Delta_2 = 0$ could be fitted to a nearly prolate ellipsoid, with half axis $a = 23.4$ Å, $b = 21.9$ Å, and $c = 53$ Å (Figure 4 and Table 1).

The structure of BSA in aqueous solution with pH ~7 and at room temperature is still controversial. SANS works report an oblate ellipsoid shape, which might be close to the "heart-shaped" structure of the crystalline HSA molecule.[8,28] The small-angle X-ray scattering (SAXS) curve of BSA in solution has even been modeled according to the atomic crystalline structure of HSA.[29] In contrast, hydrodynamic sedimentation experiments[30] and rotational time measurements[31] showed that BSA in aqueous solution adopts a prolate ellipsoidal shape (a, b, b) with $a = 20 \pm 2$ Å and $b = 70 \pm 2.5$ Å. Several small scattering experiments reported in literature have also shown that the BSA adopts a prolate ellipsoidal shape in solution.[27,28,32−34] In particular, previous SANS experiments provided a prolate ellipsoidal shape for BSA in aqueous solution, with $a = 19$ Å and $b = 68$ Å[32] or with $a = 24.2$ Å and $b = 52.2$ Å.[35]

All the results above suggest the possibility of a dynamic coexistence of various BSA conformers in solution, as previously suggested in the literature.[28] It was not possible in our work to model the SANS curve for 1 wt % BSA $\Delta_2 = 0$ according to an oblate ellipsoidal shape. Indeed, even if our results have been performed at 37 °C, the half-axis obtained from our modeling (Table 1) is in good agreement with the dimensions mentioned in the paragraph above for the prolate ellipsoidal shape at room temperature.

SANS curves for $\Delta_2 > 0$ were modeled according to an ellipsoid of revolution with two different levels of scattering length density (eqs 10−12), using SASfit software. Table 1 contains the structural parameters extracted from the modeling of the SANS curves showed in Figure 4.

According to results listed in Table 1, the BSA/PEG_{2000}−PE complexes adopt an oblate ellipsoidal shape in solution. The volume of the complexes increases with increasing PEG_{2000}−PE concentration, similarly to the amount of water contained in the core and the corona. Parameters in Table 1 describe a structure that becomes progressively more loose when the concentration of PEG−lipid in the system is increased, pointing to an unfolding effect of the PEG_{2000}−PE on the protein. It is interesting to observe that d decreases although X_{sh} increases with increasing PEG_{2000}−PE concentration. It is possible that there is a change of conformation of the PEG_{2000}−PE molecules in the external shell upon increasing $c_{PEG_{2000}-PE}$. In addition, it was not necessary to consider a contribution to the SANS from PEG_{2000}−PE micelles (Figure 3) in order to model the SANS curves in Figure 4 for $\Delta_2 > 0$. Similarly to DLS results in Figure 2, the presence of BSA in the BSA/PEG_{2000}−PE disrupts the formation of polymer−lipid conjugate micelles and favors PEG_{2000}−PE association to the protein.

According to data in Table 1, the volume of BSA at $\Delta_2 = 0$ is $V_{BSA} = 1.1 \times 10^5$ Å^3. The protein volume grows, due to BSA unfolding, from $V_{BSA} = 9.6 \times 10^4$ Å^3 for $\Delta_2 = 0.15$ to $V_{BSA} = 7.5 \times 10^5$ Å for $\Delta_2 = 2$ ($V_{BSA} = V_c$ for $\Delta_2 > 0$). However, results in Table 1 do not denote an extensive protein unfolding. The partially unfolded F-conformation adopted by BSA at pH 2.7−4.3 (roughly ellipsoidal shape with dimensions ca. 40 Å × 40 Å × 129 Å)[34,36] corresponds to $V_{BSA} = 8.8 \times 10^5$ Å^3, above the volumes obtained in this work.

To evaluate if SANS results are in good agreement with DLS results, it is possible to use Perrin's formula for an oblate ellipsoid[37] to calculate the hydrodynamic radius by using the parameters extracted from the SANS modeling:

$$R_{H,SANS} = \frac{(t+d)\gamma}{\tan^{-1}\gamma} \tag{16}$$

where $\gamma = [(s+d)^2/(t+d)^2 - 1]^{1/2}$. $R_{H,SANS}$ calculated by using the parameters listed in Table 1 is plotted in Figure 2b together with R_H. Figure 2b shows that $R_{H,SANS}$ is on average 5 Å bigger than R_H, which is a reasonable agreement in keeping with the idea that DLS data-scale is in nanometers while SANS data-scale is in angstroms (the average standard deviation for R_H, calculated by using the standard deviations for each R_H shown in Figure 2b, is 2 Å).

Figure 5 shows the Guinier plots for 1 wt % BSA and $\Delta_2 = 0-2$. The SANS curves in Figure 5 present only one Guinier

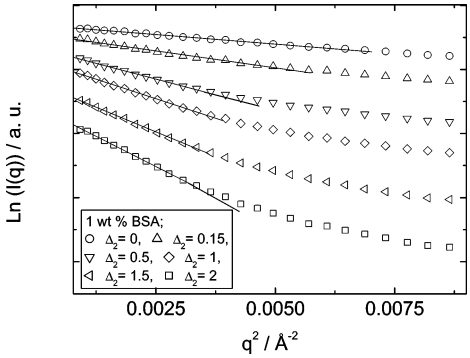

Figure 5. Guinier plots for SANS curves displayed in Figure 4. The Guinier plots have been shifted to enable the visualization of the data. The full line is the fitting according to eq 13.

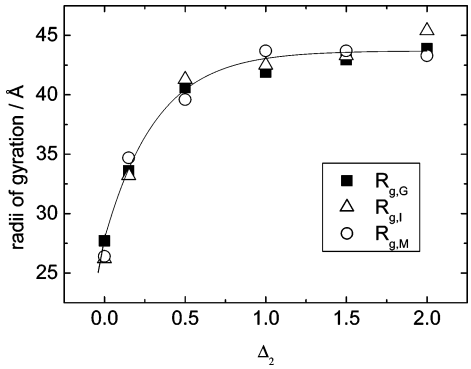

Figure 6. Dependence of the radii of gyration R_g with Δ_2. (■) $R_{g,G}$ obtained from the Guinier plots in Figure 5, (△) $R_{g,I}$ obtained from the calculation of $p(r)$, and (○) $R_{g,M}$ calculated by using the parameters obtained from the modeling in Figure 4.

region, showing that there is only one distribution of particle sizes in the system, in good agreement with our results above. The radius of gyration of the scattering particle was calculated from the fitting of eq 13 to the SANS data in Figure 5.

Figure 6 shows the dependence of $R_{g,G}$ on Δ_2. Similarly to R_H (Figure 2b), $R_{g,G}$ increases with $c_{PEG_{2000}-PE}$, from 28 Å ($\Delta_2 = 0$) to 44 Å ($\Delta_2 = 2$). The radius of gyration obtained here for $\Delta_2 = 0$ ($c_{BSA} = 1$ wt %) is similar to the room-temperature values $R_g = 30.6$ Å measured by SAXS[33] and $R_g = 30.5$ Å measured by SANS.[17]

To establish a correspondence between parameters in Table 1 and $R_{g,G}$, the radii of gyration for the oblate ellipsoids in Table 1 was calculated according to[19]

$$R_{g,M} = \left[\frac{(t+d)^2 + 2(s+d)^2}{5}\right]^{1/2} \qquad (17)$$

The resulting $R_{g,M}$ are plotted in Figure 6 and show an excellent agreement with $R_{g,G}$.

The distance distribution function of the system $p(r)$ was calculated with the program GNOM,[38] for 1 wt % BSA and $\Delta_2 = 0-2$. Some representative results obtained for $p(r)$ are shown in Figure 7, while the inset in Figure 7 compares the Δ_2-dependence of D_{max} and the maximum distance of the ellipsoids in Table 1, $2(s + d)$. $p(r)$ for $\Delta_2 = 0$ displays a maximum at ~31 Å and has $D_{max} = 75$ Å, in excellent agreement with previous SANS and SAXS results in the literature.[8,29] Figure 7 shows that the overall shape of the BSA/PEG_{2000}−PE complexes remains globular upon increasing Δ_2, while D_{max} smoothly increases with Δ_2. The data in the inset show that D_{max} and $2(s + d)$ are comparable quantities, since they only present an averaged 8% difference over the entire Δ_2 interval investigated.

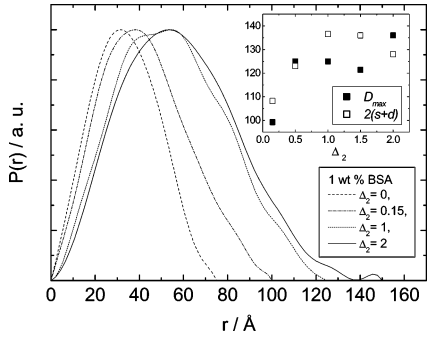

Figure 7. Distance distribution function $p(r)$ calculated for samples containing 1 wt % BSA and (---) $\Delta_2 = 0$, (·-·) $\Delta_2 = 0.15$, (···) $\Delta_2 = 1.0$, or (−) $\Delta_2 = 2.0$. The inset shows the dependence of (■) D_{max} and (□) 2(s+d) with Δ_2.

Finally, $R_{g,I}$ calculated through eq 15 is plotted in Figure 6 together with $R_{g,M}$ and $R_{g,G}$. Results in Figure 6 support the consistency of the SANS modeling on the basis of the good agreement between the size of the particle calculated imposing a particular geometry ($R_{g,M}$) and the overall size of the particle calculated without imposing geometrical restrictions ($R_{g,I}$ and $R_{g,G}$).

Conclusions

In this work we have reported a structural study of BSA/PEG_{2000}−PE complexes in solution for $\Delta_1 = 0-60$ ($c_{BSA} = 0.01$ wt %, UV experiments) and $\Delta_2 = 0-2$ ($c_{BSA} = 1$ wt %, DLS, SLS, and SANS experiments).

UV results show that at $\Delta_1 = 0.15$ the Trp groups on the BSA surface are in contact with the PEG−lipid conjugate, while for $\Delta_1 > 0.15$ the Trp groups are exposed to water. According to UV intensity, BSA unfolding starts at $\Delta_1 = 0.15$, with concentrations as low as $c_{PEG_{2000}-PE} = 0.0015$ wt %. Therefore, UV results put forward the hypothesis of a protein/polymer−lipid conjugate network extended throughout the sample due to BSA unfolding for $c_{PEG_{2000}-PE} > 0$.

DLS, SLS, and SANS were used to rule out the hypothesis above, pointing out the existence of individual BSA/PEG−lipid complexes in the system. DLS shows that the there is only one BSA molecule per complex, while SLS shows that the PEG−lipid associates to the BSA without promoting aggregation between adjacent protein/polymer−lipid conjugate complexes. SANS was used to show that the complexes adopt an oblate ellipsoidal shape consisting of an inner core, containing the BSA, surrounded by an external shell where the PEG_{2000}−PE is located. SANS also proved that BSA does not undergo a fully extended unfolding for $\Delta_2 > 0$, attaining dimensions lower than the partially unfolded F-conformation adopted by the BSA at pH 2.7−4.3.[34]

The results presented in this work are enough to prove that BSA/PEG_{2000}−PE complexes can potentially be used to control the osmotic blood pressure. This statement is supported by the individual BSA/PEG_{2000}−PE complexes which can be identified in the system. The absence of extended protein/polymer−lipid networks in the solution will not induce any undesirable blood dysfunction. The tertiary structure of the BSA is not fully unfolded under association with the PEG_{2000}−PE, while each complex probably presents an individual BSA macromolecule trapped in a PEG_{2000}−PE shell. The presence of one BSA monomer per each BSA/PEG_{2000}−PE complex does not favor

a potential aggregation of BSA into clusters, which could lead to inhomogeneous domains in the blood stream.

Acknowledgment. V.C. would like to acknowledge Prof. J. Gibbins for providing the facilities for the UV experiments and Prof. I. W. Hamley for giving access to the light scattering machine. V.C. and L.A.C. would like to acknowledge Dr. J. Kohlbrecher for several discussions about his SASfit program. V.C. was supported by a UK Relocation Fellowship from the Royal Society.

References and Notes

(1) Delgado, C.; Francis, G. E.; Fisher, D. *Crit. Rev. Ther. Drug Carrier Syst.* **1992**, *9*, 249.
(2) Assaly, R. A.; Azizi, M.; Kennedy, D. J.; Amauro, C.; Zaher, A.; Houts, F. W.; Habib, R. H.; Shapiro, J. I.; Dignam, J. D. *Clin. Sci.* **2004**, *107*, 263.
(3) Murthy, N. S.; Knox, J. R. *Biopolymers* **2004**, *74*, 457.
(4) Castelletto, V.; Kelarakis, A.; Krysmann, M. J.; Jauregi, P. *Biomacromolecules* **2007**, *8*, 2244.
(5) Riley, D. P.; Oster, G. *Discuss. Faraday Soc.* **1951**, *11*, 107.
(6) Doherty, P.; Benedek, G. B. *J. Chem. Phys.* **1974**, *61*, 5426.
(7) Bendedouch, D.; Chen, S.-H. *J. Phys. Chem.* **1983**, *87*, 1473.
(8) Lee, C. T.; Smith, K. A.; Hatton, T. A. *Biochemistry* **2005**, *44*, 524.
(9) Tandford, C.; Swanson, S. A.; Shore, W. S. *J. Am. Chem. Soc.* **1955**, *77*, 6414.
(10) Putnam, F. W. *The Plasma Proteins*; Academic Press: New York, 1960.
(11) Berne, B. J.; Pecora, R. *Dynamic Light Scattering*; Wiley-Interscience: New York, 1976.
(12) Provencher, S. W. *Makromol. Chem.* **1979**, *180*, 201.
(13) Guinier, A. *X-ray Diffraction*; W. H. Freeman: San Francisco, CA, 1963.
(14) Kotlarchyk, M.; Chen, S.-H. *J. Chem. Phys.* **1983**, *79*, 2461.
(15) Bergström, M.; Pedersen, J. S. *Phys. Chem. Chem. Phys.* **1999**, *1*, 4437.
(16) Marignan, J.; Bassereau, P.; Delord, P. J. *J. Phys. Chem.* **1986**, *90*, 645.
(17) Bendedouch, D.; Chen, S.-H. *J. Phys. Chem.* **1983**, *87*, 1473.
(18) Guinier, A.; Fournet, G. *Small-Angle Scattering of X-rays*; John Wiley & Sons, Inc.: New York, 1955.
(19) Glatter, O.; Kratky, O. *Small Angle X-ray Scattering*. Academic: London, UK, 1982.
(20) Teramoto, A.; Takagi, Y.; Hachimori, A.; Abe, K. *Polym. Adv. Technol.* **1999**, *10*, 681.
(21) Deep, S.; Ahluwalia, J. C. *Phys. Chem. Chem. Phys.* **2001**, *3*, 4583.
(22) Antonov, Y. A.; Wolf, B. A. *Biomacromolecules* **2005**, *6*, 2980.
(23) Papadopoulou, A.; Gree, R. J.; Frazier, R. A. *J. Agric. Food Chem.* **2005**, *53*, 158.
(24) Azegami, S.; Tsuboi, A.; Izumi, T.; Hirata, M.; Dubin, P. L.; Wang, B.; Kokufuta, E. *Langmuir* **1999**, *15*, 940.
(25) Harvey, J. D.; Geddes, R.; Wills, P. R. *Biopolymers* **1979**, *18*, 2249.
(26) van Dijk, J. A. P. P.; Smit, J. *J. Chromatogr. A* **2000**, *867*, 105.
(27) Reščič, J.; Vlachy, V.; Jamnik, A.; Glatter, O. *J. Colloid Interface Sci.* **2001**, *239*, 49.
(28) Kiselev, M.; Gryzunov, I. A.; Dobretsov, G. E.; Komarova, M. N. *Biofizika* **2001**, *46*, 423.
(29) Santos, S.; Zanette, D.; Fischer, H.; Itri, R. *J. Colloid Interface Sci.* **2003**, *262*, 404.
(30) Squire, P. G.; Moser, P.; O'Konski, C. T. *Biochemistry* **1968**, *7*, 4261.
(31) Wright, A. K.; Thompson, M. R. *Biophys. J.* **1975**, *15*, 137.
(32) Sjoeberg, B.; Mortensen, K. *Biophys. Chem.* **1997**, *65*, 75.
(33) Luzzati, V.; Witz, J.; Nicolaieff, A. J. *J. Mol. Biol.* **1961**, *3*, 379.
(34) Bloomfield, V. *Biochemistry* **1966**, *5*, 684.
(35) Das, A.; Chitra, R.; Choudhury, R. R.; Ramanadham, M. *Pramana* **2004**, *63*, 363.
(36) Carter, D. C.; Ho, J. X. In *Advances in Protein Chemistry*; Schumaker, V. N., Ed.; Academic Press: Los Angeles, CA, 1994.
(37) Perrin, F. *J. Phys. Radium* **1936**, *7*, 1.
(38) Svergun, D. I. *J. Appl. Crystallogr.* **1992**, *25*, 495.